From FA Smith, Applied Radiation Physics

1.6 Synchrotron Radiation

The earliest circular-orbit electron accelerators were energy-limited because of the emission of synchrotron radiation. Higher energies could be achieved only through the insertion of a number of rf accelerating gaps round the electron orbit. These additional accelerating gaps, together with the magnet structure in Fig.(1.27), resulted in the electron synchrotron. The machine quickly became adapted to the sole purpose of generating this radiation which spans a continuous range from the infra-red (eV) to hard X-rays (10^5 eV).

Like any other source of electromagnetic radiation, synchrotron radiation can be characterized by its :

- energy (or wavelength),
- spectral brightness (expressed in photons s^{-1} mm^{-2} mr^{-2} (0.1% bandwidth)$^{-1}$),
- polarization (defined by the plane of oscillation of the electric vector),
- coherence (the phase relation between photons),
- emittance (extent of angular divergence and finite size of the source).

Complete details of the foundation of synchrotron radiation sources can be found in the proceedings of recent international conferences and summer schools [13],[14],[15],[16] and [17].

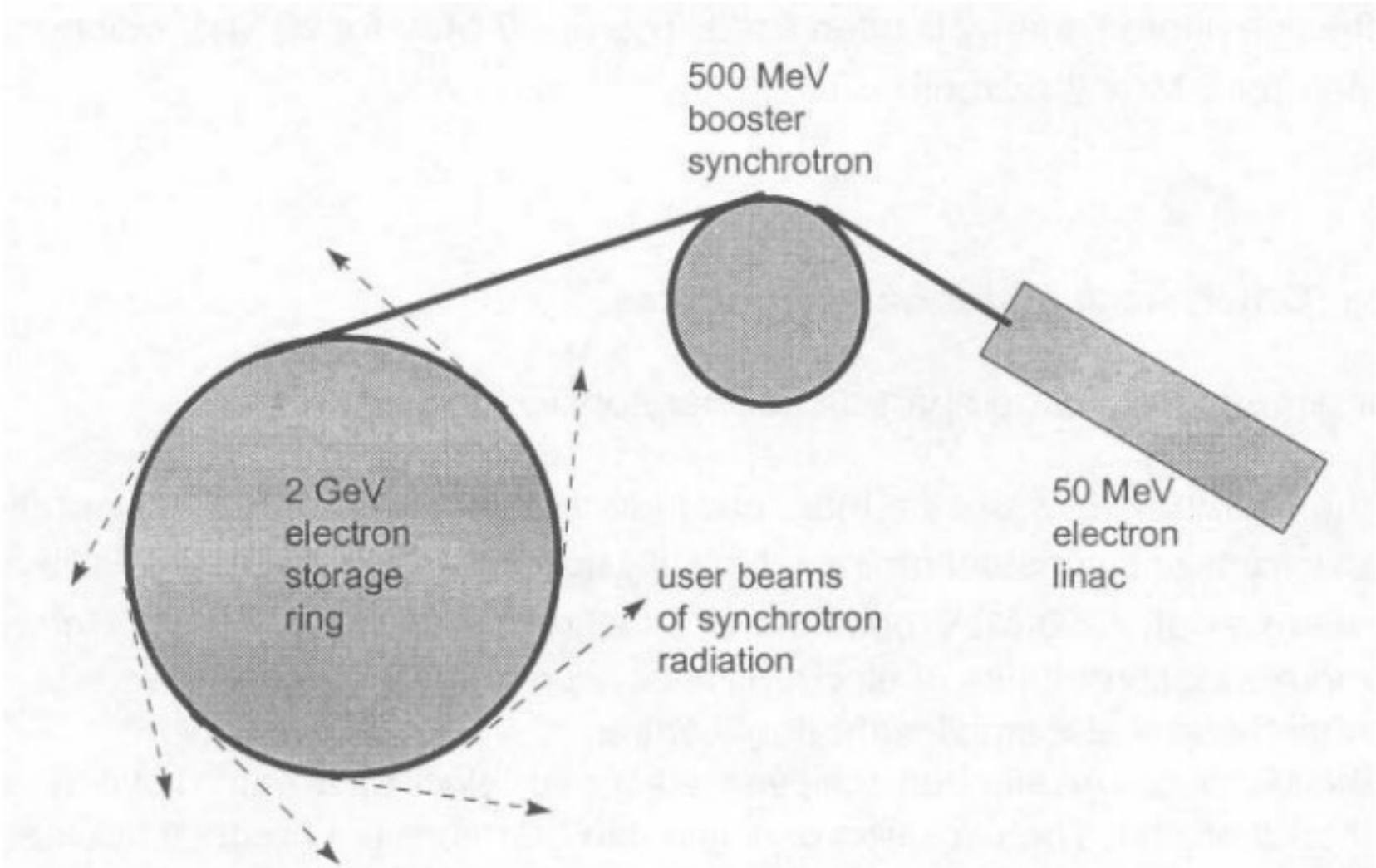

Fig. (1.27) A typical electron storage ring used to produce synchrotron radiation.

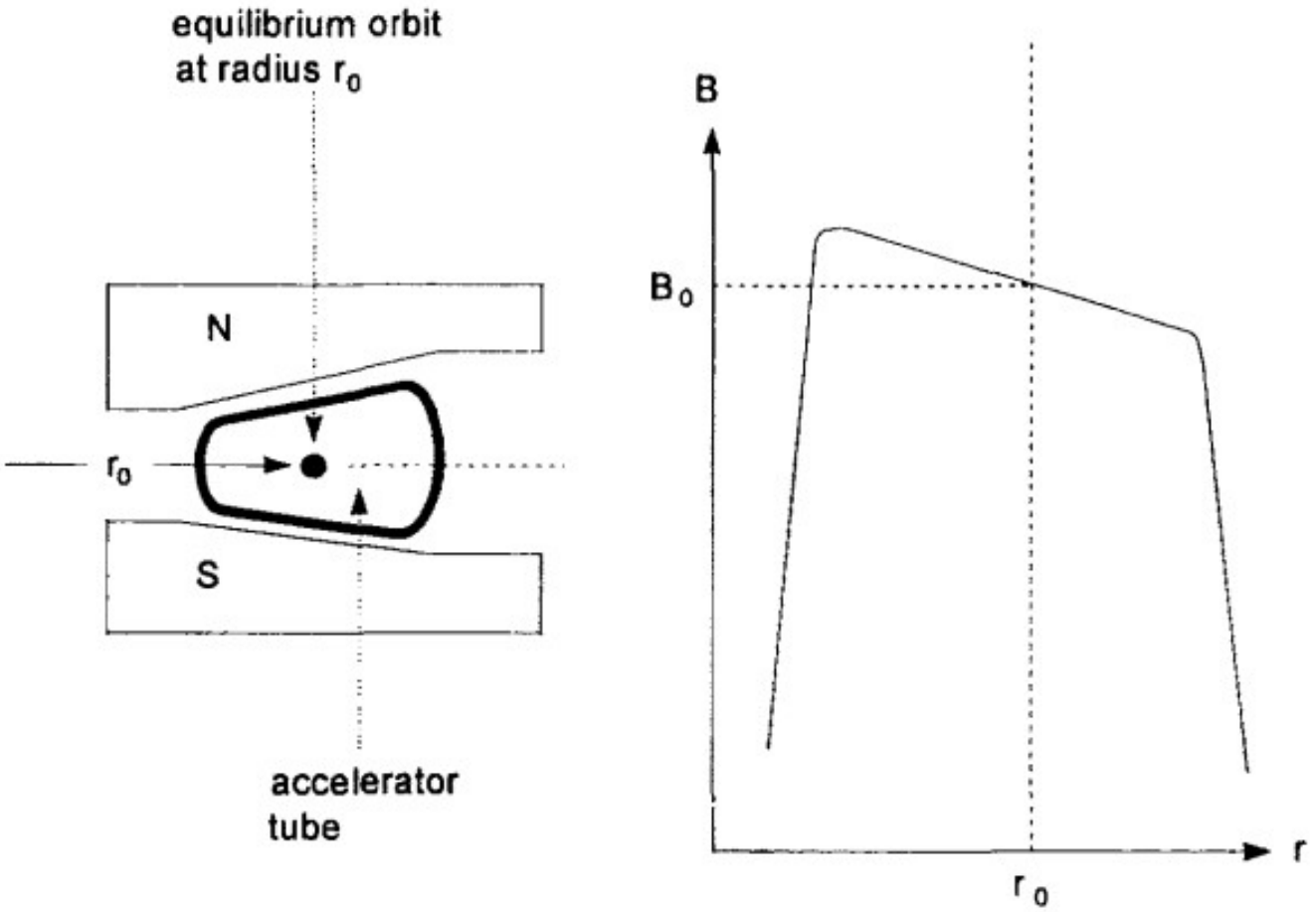

Fig.(1.28) A sketch of the radial decrease in field at the equilibrium orbit brought about by the shaping of the magnet poles, [7].

The energy distribution of photons emitted in synchrotron radiation is determined by the energy of the electron and its orbit radius. It is described in the first instance by the characteristic photon energy, ε_c. This is defined as the central energy which divides the emitted power distribution into two halves. When the electron energy is normalized to its rest energy, we have γ = electron energy/m_0c^2, where m_0 is the electron rest mass and :

$$\varepsilon_c = \hbar\omega_c = \frac{\hbar 3c\gamma^3}{2\rho} \qquad (1.20)$$

The instantaneous radius of the electron path, ρ, is equal to the equilibrium synchrotron radius, r_0, except when sinusoidal magnetic structures, Fig.(1.29), are inserted into the storage ring. Expressing ε_c in keV we have :

$$\varepsilon_c = \hbar\omega_c = h\nu_c = 2.218\frac{E^3}{r_0} = 0.665E^2B \qquad (1.21)$$

In Eq.(1.21), E is the electron beam energy in GeV, B is the magnetic field in Tesla and r_0 is the orbit radius in metres. A 2 GeV beam energy and a 20 m radius therefore has a characteristic photon energy of 887 eV with a wide distribution of photon energies about this value.

Conservation of momentum requires that the radiation is emitted in a narrow cone-shaped beam tangential to the orbit. The nominal angular width of this cone is $\sim 1/\gamma$. Furthermore, the polarization is linear, with an electric vector which is horizontal when observed in the plane of the bending magnets.

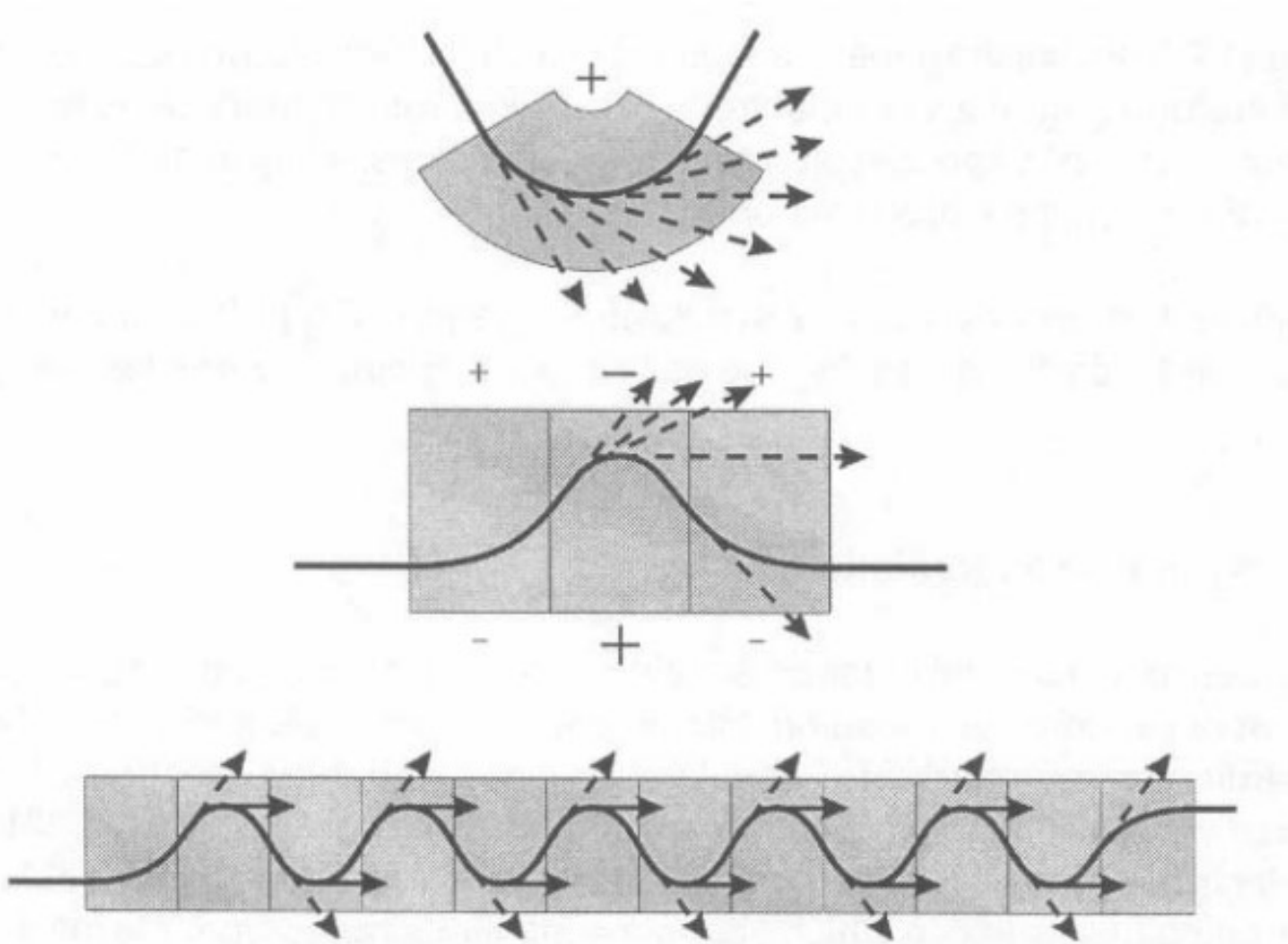

Fig.(1.29) Types of magnet structures used for imposing sinusoidal variations onto the otherwise circular electron orbit.

1.6.1 *Polarization*

A general expression for the double differential angular distribution of photon flux, f_s, within, and perpendicular to, the electron orbit plane [14] is :

$$\frac{d^2 f_s}{d\theta d\psi} = \frac{3\alpha}{4\pi^2}\gamma^2 \frac{\Delta\omega}{\omega}\frac{I}{e}\left(\frac{\omega}{\omega_c}\right)^2 \left(1+\gamma^2\psi^2\right)^2\left[K_{2/3}^2(x) + \frac{\gamma^2\psi^2}{1+\gamma^2\psi^2}K_{1/3}^2(x)\right] \qquad (1.22)$$

In Eq.(1.22), $x = \omega(1+\gamma^2\psi^2)^{3/2}/2\omega_c$, $\alpha \cong 1/137$ is the fine structure constant, I is the beam current, and θ and ψ are the angles of observation in the horizontal and vertical planes respectively. The $K_{2/3}(x)$ and $K_{1/3}(x)$ terms are Bessel functions of the second kind and refer to the horizontal and vertically polarized intensity components. These are illustrated graphically in Fig.(1.31).

Consider a beam energy of 2 GeV and a photon energy of $\varepsilon/\varepsilon_c = 0.01$. An abscissa value of 4 in Fig.(1.31) gives an observation angle of $\psi = 4\times 0.511/2000 = 1.02 \times 10^{-3}$ mrad. out of the horizontal plane. The normalized vertical and horizontal intensities in this case are 37% and 65% respectively. The major : minor axes of the polarization ellipse are therefore given by the square root of the ratio of intensities 1.33 : 1.

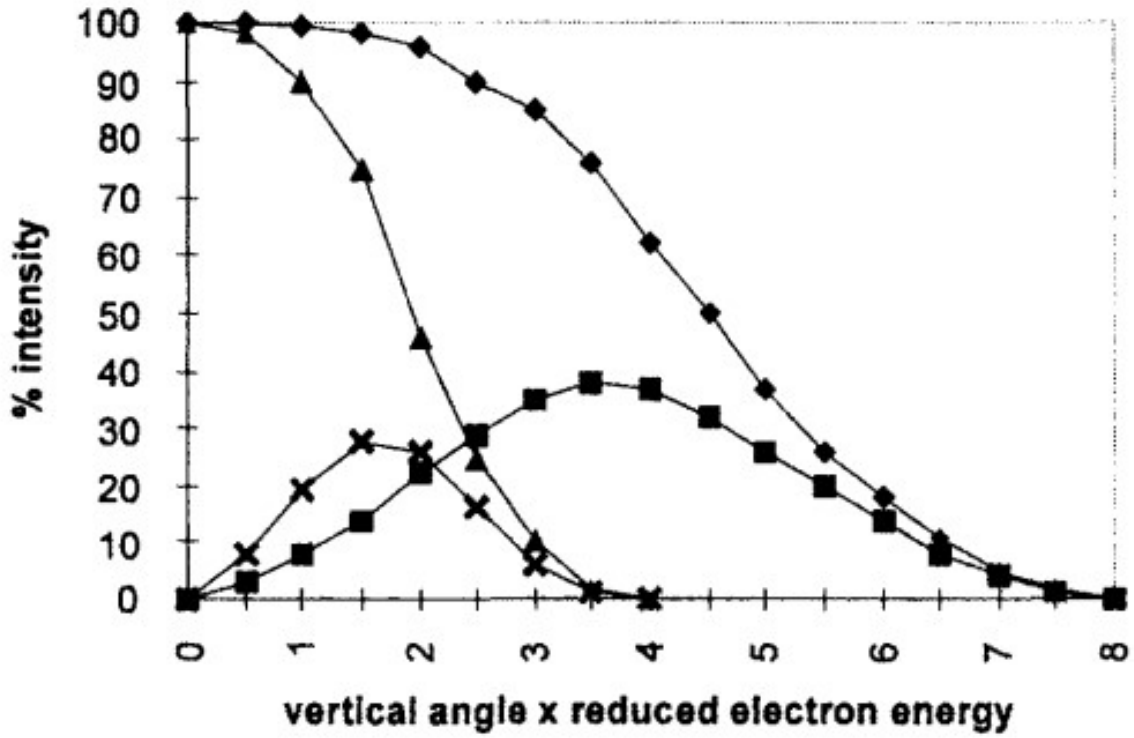

Fig.(1.31) Percentage intensity of horizontal and vertically polarized photons versus the product of vertical observation angle ψ and the reduced electron energy γ. ◆ $\varepsilon/\varepsilon_c$ = 0.01 horizontal : ■ $\varepsilon/\varepsilon_c$ = 0.01 vertical : ▲ $\varepsilon/\varepsilon_c$ = 0.1 horizontal : ✖ $\varepsilon/\varepsilon_c$ = 0.1 vertical, [17].

1.6.2 *Coherence*

The use of periodic magnetic structures requires the definition of a deflection parameter K. This is expressed as :

$$K = \frac{eB_0\lambda_u}{2\pi m_0 c} = 0.934\lambda_u B_0 \qquad (1.23)$$

where the magnetic field, perpendicular to the electron orbit, varies sinusoidally along the z axis with a maximum value of B_0 and a period of λ_u. Thus :

$$B = B_0 \sin\left(2\pi \frac{z}{\lambda_u}\right)$$

where B_0 is in Tesla, and λ_u is in cm. The maximum angular deflection of the orbit is given by $\delta = K/\gamma$.

The deflection parameter K provides the distinction between the two types of periodic magnet structures [17] :

- Wiggler structures have $K > 1$, when radiation from the different parts of the trajectory add incoherently. If there are N magnet periods, the total photon flux produced is $2N$ times the expression for a bending magnet, Eq.(1.22). The polarization will always be linearly polarized.
- Undulator structures have $K \leq 1$. In this case the deflection angles are within the cone angle $1/\gamma$. The radiation from each period then adds coherently to give a strong fundamental with its weaker harmonics.

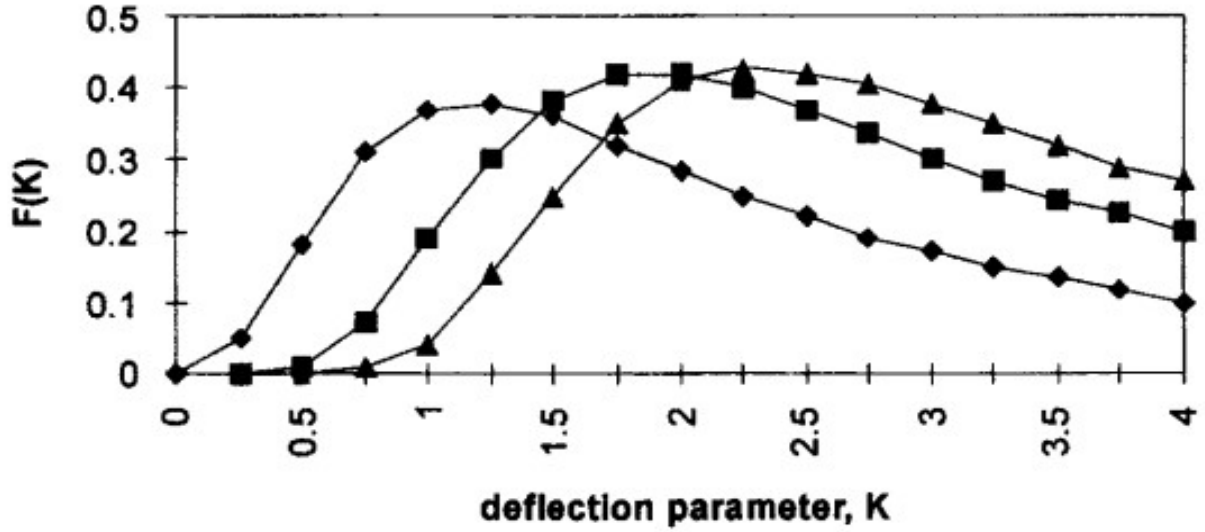

Fig.(1.32) The function $F_n(K)$, Eq.(1.27), for n = 1 (◆): n = 3 (■): n = 5 (▲), [17].

The wavelength of the fundamental radiation measured on the axis of an undulator (when $\theta = \psi = 0$) is :

$$\lambda_1 = \frac{\left(1 + K^2 / 2\right)}{2\gamma^2}\lambda_u = \frac{13.056\lambda_u}{E^2}\left(1 + \frac{K^2}{2}\right) \qquad (1.24)$$

where E is the electron energy in GeV and λ_u is the undulator period in cm. The corresponding energy in keV is :

$$\varepsilon_1 = 0.950\frac{E^2\lambda_u}{\left(1 + K^2 / 2\right)} \qquad (1.25)$$

and the fractional bandwidth for order n is :

$$\frac{\Delta\varepsilon}{\varepsilon} \cong \frac{1}{nN} \qquad (1.26)$$

On the axis, the differential angular distribution of photon flux is non-zero only for odd orders (n = 1,3,5..). In the orbit plane ($\psi = 0$) we have :

$$\frac{d^2 f_s}{d\theta d\psi} = \alpha N^2 \gamma^2 \frac{\Delta\omega}{\omega} \frac{I}{e} F_n(K) \qquad (1.27)$$

The function $F_n(K)$ is given for orders n = 1,3 and 5 in Fig.(1.27).

When Eq.(1.27) is expressed in practical units it becomes :

$$\frac{d^2 f_s}{d\theta d\psi} = 1.74 \times 10^{14} N^2 I F^2 F_n(K) \qquad (1.28)$$

1.6.3 Emittance

Eqs.(1.22) and (1.28) overestimate the photon flux because of the finite source size and the finite angular divergence. Emittance is specified in both horizontal (x) and vertical (y) planes by the product of the root mean square (rms) beam size $\sigma_x \sigma_y$ and the beam divergence $\sigma_{x'} \sigma_{y'}$. For the two planes therefore :

$$\varepsilon_x = \sigma_x \sigma_{x'} \quad \varepsilon_y = \sigma_y \sigma_{y'}$$

However, emittance is only one of a number of factors needed to convert photon flux to brightness β. The latter is defined as photon flux per unit phase-space volume. It requires a consideration of the transverse and longitudinal coherence in defining the effective source area [15]. Thus :

$$\beta = \frac{d^2 f_s}{d\theta d\psi} \Big/ (\text{effective source area})$$

Table (1.3) Calculated parameters of synchrotron beams at 6 GeV electron energy and 100 mA storage ring current [13]. Note the small value of K for the undulator brought about by the large number of small period oscillations. Energy values in column 8 refer to the characteristic photon energy for the bend and wiggler magnets and the fundamental energy for the undulator.

Source	σ_x (mm)	σ_y (mm)	N	λ_u (cm)	K	B_0 (T)	ε_c or ε_1 (keV)	β
bend	0.34	0.14	-	-	-	1.0	23.94	2.3×10^{14}
wiggler	0.34	0.14	4	34	57.1	1.8	43.10	1.8×10^{15}
undulator	0.34	0.14	344	1.6	0.200	0.13	20.9	2.5×10^{17}

1.7 Neutron Sources

Although neutrons can be produced spontaneously by the radioactive decay of certain heavy nuclei (section 1.3.4), their principal means of production uses either a nuclear reactor or an accelerator-based reaction process.

1.7.1 Reactors

Reactors can be used for :

- isotope production (see chapter 8),
- industrial radiography,
- boron neutron capture therapy (BNCT) (see chapter 9),
- providing neutron beams for research.

The main components and processes inside the reactor, Fig.(1.33), are :

- the induced fission of fissile material (fuel : ^{235}U, ^{239}Pu for thermal fission and ^{238}U for fast fission). In a fast reactor, the fission takes place at high (> MeV) energies. In a thermal reactor, the spectrum of neutrons released in the fission process, Fig.(1.7), must be degraded to thermal energies in order to initiate further fission. The energy degradation is achieved by the moderator.
- the moderator. This is composed of light nuclei (H_2O, D_2O, C) with which the energetic neutrons collide and lose energy. These collisions are elastic in the centre-of-mass co-ordinate system. The neutron loses energy in the laboratory system because of the recoil of the struck nucleus.
- the coolant system. Kinetic energy imparted to all the fission products – neutrons, fission fragments and their decay products – is recovered by a coolant system. This energy can then be converted into usable heat.

As a source of radiation the nuclear reactor is primarily a source of neutrons. The induced-fission spectrum of neutrons emitted from the fuel rods is the same as the spectrum from a spontaneous-fission radioactive source, Fig.(1.7), Eq.(1.12).

In a thermal reactor, the moderator degrades the energy spectrum. It comprises:

- a Maxwell-Boltzmann distribution in equilibrium with the core temperature. This describes the neutrons already thermalized and,
- a slowing down (1/E) component which results from the continual moderation of neutrons from the fission spectrum, Fig.(1.34).

A crucial factor in the operation of a nuclear reactor is the production of fission fragments – the two heavy elements into which the original fuel nucleus has been split. In binary fission, these fragments have a yield distribution shown in Fig.(1.35).

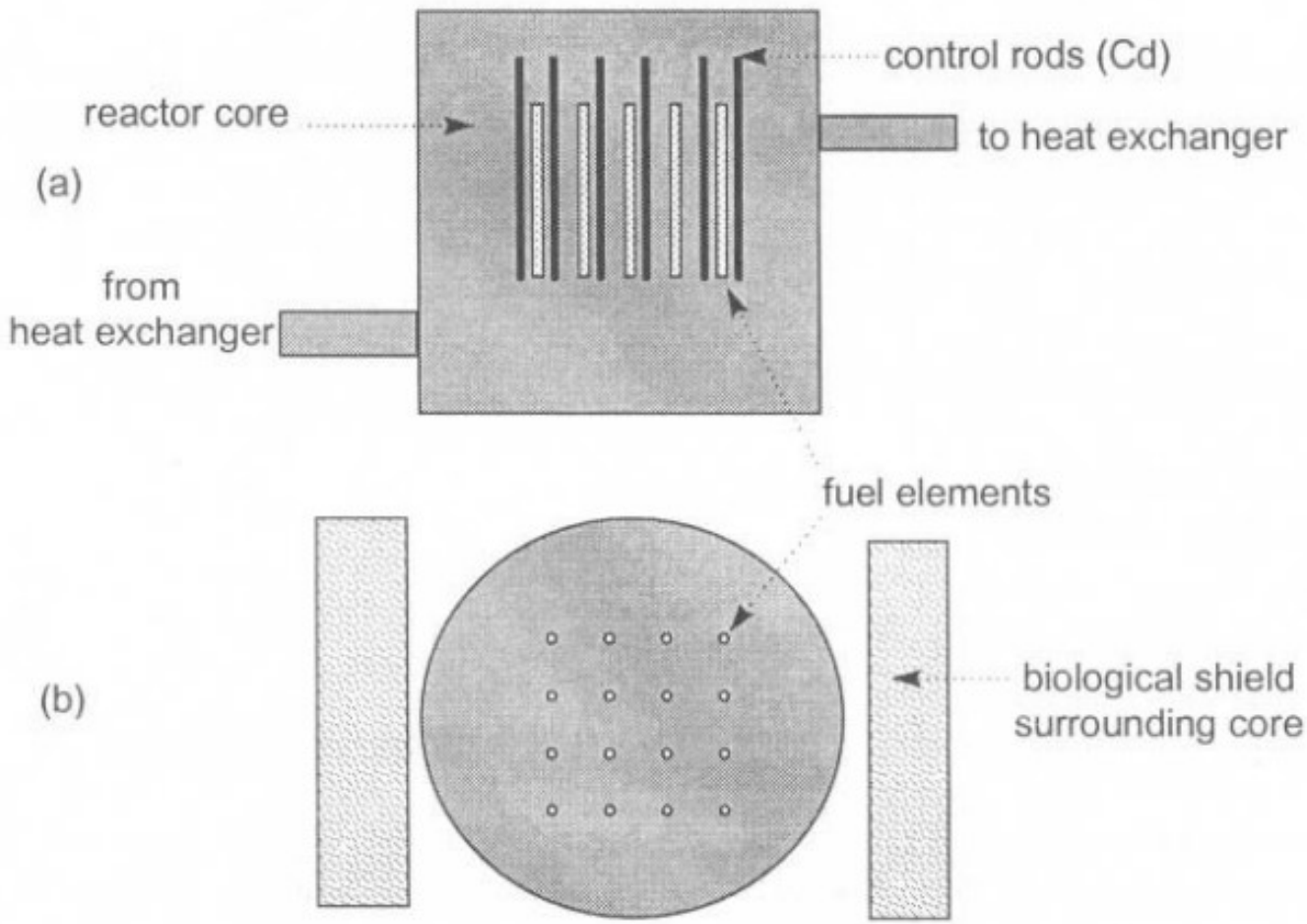

Fig.(1.33) A schematic diagram of a reactor core. Moveable control rods, which have a high thermal neutron absorption cross section, are interspersed within a lattice of fuel rods. The positioning of these rods allows the neutron flux to be held at a constant value, called the criticality condition. Rods fully withdrawn will allow the neutron flux to rise exponentially. In this event the reactor becomes super-critical. When fully inserted, the flux falls exponentially to give the sub-critical condition.

The radioactive decay of these fission-fragments results in :

- prompt γ-rays,
- delayed neutrons (mainly from the decay of isotopes of bromine and iodine),
- decay γ-rays.

There is a wide variety of fission fragments whose decay gives rise to delayed neutrons. These are generally grouped together on the basis of their decay half-life, Table (1.4). Typical examples of fission-fragment decays in groups 2 and 3 are :

$$^{87}\mathrm{Br} \xrightarrow{\beta 5.56\mathrm{s}} {}^{87}\mathrm{Kr} \xrightarrow{n} {}^{86}\mathrm{Kr}$$

$$^{137}\mathrm{I} \xrightarrow{\beta 22\mathrm{s}} {}^{137}\mathrm{Xe} \xrightarrow{n} {}^{136}\mathrm{Xe}$$

Table (1.4) The 6 major groups of delayed neutrons following the fission of ^{235}U. The groups are classified according to their β-decay half-lives. It is these neutrons which permit the control of criticality in the reactor.

Group	Half-life (s)	Decay constant λ_i (s^{-1})	Mean energy (keV)	Yield (n/fission)	Fraction β_i
1	55.72	0.0124	250	0.00052	0.000215
2	22.72	0.0305	560	0.00346	0.001424
3	6.22	0.111	405	0.00310	0.001274
4	2.30	0.301	450	0.00624	0.002568
5	0.610	1.14	-	0.00182	0.000748
6	0.230	3.01	-	0.00066	0.000273
Total				0.0158	0.0065

1.7.2 Neutrons from charged-particle reactions

Many of the charged-particle-induced reactions used for activation (Chapter 8) have a neutron as the exiting particle. Some of these were used intensively in the past for neutron cross-section determinations and for the production of neutron beams for radiotherapy. Because neither of these activities are currently widespread, most radio-isotopes that could be (intentionally) produced by neutron activation are now approached via different – charged particle – routes. Although neutron beams *per se* are no longer popular, it is essential that charged-particle reactions are considered because of their importance in radiation protection.

Most importance attaches to neutron production by heavy charged particles – mainly protons, deuterons, α-particles. Electrons are important only in so far as they can produce *bremsstrahlung* photons in dense and high atomic-number materials. These can then produce neutrons via photo-neutron reactions.

A basic requirement in a charged-particle-induced reaction is to produce a compound nucleus with an amount of excitation energy which exceeds the binding energy of the "last neutron" (see sections 8.1 and 4.2.2). This neutron is then very likely to be ejected from the compound nucleus. The Q-value of a reaction is defined as :

$$Q = \left[\left(m_p + m_t\right) - \left(m_n + m_r\right)\right]c^2 \; / \; 2$$

where the masses of the projectile, target, exiting and residual nuclei are m_p, m_t, m_n, and m_r respectively.

Some examples of the most common charged-particle-induced reactions, with their associated Q-values, are :

- (p,n): ^{7}Li (p,n) ^{7}Be : Q = - 1.646 MeV
  ^{3}H (p,n) ^{3}He : Q = - 0.764 MeV
- (d,n): ^{9}Be(d,n)^{10}B : Q = + 4.362 MeV
  ^{3}H (d,n)^{4}He : Q = + 17.588 MeV
  ^{2}H (d,n)^{3}He : Q = + 3.265 MeV

For a given reaction, it is necessary to define the relation between the Q-value and the following :

- the energies of the incoming particle, E_p, and the outgoing neutron, E_n,
- the energy given to the residual nucleus, E_r,
- the angles of emission of the neutron and the recoil nucleus with respect to the direction of the incoming particle, θ and φ respectively.

Conservation of energy and momentum for (a) non-relativistic energies and (b) for the case where no excitation energy is given to the residual nucleus, then gives:

$$\begin{aligned} E_p + Q &= E_n + E_r \\ \sqrt{2m_pE_p} &= \sqrt{2m_nE_n}\cos\theta + \sqrt{2m_rE_r}\cos\varphi \\ 0 &= \sqrt{2m_nE_n}\sin\theta - \sqrt{2m_rE_r}\sin\varphi \end{aligned} \qquad (1.29)$$

Eqs.(1.29) can be combined to give the Q-equation, [18] :

$$Q = E_n\left(1+\frac{m_n}{m_r}\right) - E_p\left(1-\frac{m_p}{m_r}\right) - \frac{2\sqrt{m_p E_p m_n E_n}}{m_r}\cos\theta \qquad (1.30)$$

Since Eq.(1.30) is quadratic in $\sqrt{E_n}$ it can be solved to give the useful relation :

$$E_n = E_p \frac{m_p m_n}{(m_n+m_r)^2}\left\{\begin{array}{l} 2\cos^2\theta + \dfrac{m_r(m_r+m_n)}{m_p m_n}\left[\dfrac{Q}{E_p}+\left(1-\dfrac{m_p}{m_r}\right)\right] \\ \pm 2\cos\theta\sqrt{\cos^2\theta + \dfrac{m_r(m_r+m_n)}{m_p m_n}\left[\dfrac{Q}{E_p}+\left(1-\dfrac{m_p}{m_r}\right)\right]} \end{array}\right\} \qquad (1.31)$$

Eq.(1.31) is a general relation for any angle of neutron emission, θ, and for $Q > 0$ (exothermic) or $Q < 0$ (endothermic) reactions. Only the positive sign is used for exothermic reactions (otherwise it could give $E_n > E_p$ at $\theta = 0$ when the negative sign is used, which is energetically not possible). In this case there is a unique relation between E_n , E_p and θ .

Neutron energies from endothermic reactions are governed by a threshold incident particle energy given by :

$$E_{p,threshold} = |Q| \frac{m_p + m_t}{m_t} \tag{1.32}$$

When $E_p < E_{p,threshold}$ there is no reaction. When $E_p = E_{p,threshold}$ the reaction products are just formed with zero energy in the CM system, but they move forward with the velocity of the centre of mass in the laboratory system. As $E_p > E_{p,threshold}$, two neutron energies are produced, one for the negative and one for the positive sign in Eq.(1.31). These are emitted within a cone of semi-angle :

$$\cos\theta = \left| \sqrt{\frac{m_r(m_n + m_r)}{m_p m_n} \left[\frac{|Q|}{E_p} - \left(1 - \frac{m_p}{m_r} \right) \right]} \right| \tag{1.33}$$

Eventually, E_p will become so large that the lower neutron energy becomes zero, at which point only the positive sign is used in Eq.(1.31) to give a mono-energetic neutron [18].

Eq.(1.31) shows that for a given reaction, and for given values of E_p and θ, a mono-energetic neutron is produced. This applies to the ideal case of an infinitely thin target in which there is no energy degradation of the incident charged particle. In practice, of course, the incident particle will lose energy and may also scatter. The resulting neutron spectrum is therefore determined by :

- the energy spread of charged particles from the accelerator which impinge on the target. This will generally be small (~ 5%),
- the energy-dependent cross-section, $\sigma_{d,n}(E_p)$(see also section 8.4),
- the thickness of the target, d, compared with the range of the incident charged particle in the target material, R. If R < d then neutron production can take place at all energies between the incident energy E_p and zero for $Q > 0$, and between E_p and $E_{p,threshold}$ for $Q < 0$.

1.7.3 Neutrons from photon-induced reactions

The main characteristics of a neutron source based on photo-neutron reactions are:

- they are always endo-thermic ($Q < 0$) because of the mass-less incident particle,
- photo-neutron cross-sections are much smaller than those using charged particles. The yield (neutrons/incident photon) is therefore less,
- the incident photons are never completely stopped in the target. This means that there is always a residual photon background.

Photoneutron sources can use either γ-rays from a radioactive source (section 1.3.2) or energetic *bremsstrahlung* X-rays from an electron accelerator (section 1.4.4).

The excitation energy of the compound nucleus of the target must exceed the binding energy of the least-bound neutron before neutron emission can take place. Radioactive (γ,n) sources are therefore restricted to targets which have the smallest binding energy. These are deuterium (Q = - 2.225 MeV) and beryllium (Be^9, Q = - 1.665 MeV).

Bremsstrahlung-based sources will generally use high-Z targets which must be capable of withstanding the high power density of the incoming electron beam.

For these reasons, tungsten and gold are preferred. However, an increased yield can be obtained through the use of a secondary, fissile, target. In this case the photons produced in the primary (tungsten) target produce photo-fission reactions in the secondary (usually uranium) target.

Conservation of energy and momentum in the reaction gives

$$h\nu - |Q| = E_n + E_r$$
$$\frac{h\nu}{c} = m_n v_n - m_r v_r \qquad (1.34)$$

in the special case where the neutron is emitted at 0° to the direction of the incident photon, Eq.(1.29).

The equivalent expression for photo-neutron reactions to Eq.(1.31) for charged particle reactions is, [18] :

$$E_n = \frac{A-1}{A}[h\nu - |Q|] \pm h\nu\sqrt{\frac{2(A-1)\times[h\nu - |Q|]}{931\times A^3}} \qquad (1.35)$$

where A is the atomic number of the target material. Since the factor 931 is the approximate energy equivalent in MeV of one atomic mass unit, the energies of E_n, $h\nu$ and Q must also be expressed in MeV.

Eq.(1.35) shows that the fractional energy spread of neutrons emitted along the line of an incident mono-energetic photon is given by :

$$\frac{\Delta E_n}{E_n} = \frac{2h\nu\sqrt{\dfrac{2(A-1)\times\left[h\nu-|Q|\right]}{931\times A^3}}}{\dfrac{(A-1)}{A}\left[h\nu-|Q|\right]} \tag{1.36}$$

A 2 MeV incident photon on a ^{9}Be target will thus give a neutron energy of 0.3 MeV at an emission angle of 0°. The fractional energy spread is 0.0112/0.3 ≈ 4%. In practice, of course, a much larger energy spread is observed because of the variation of Eq.(1.34) at different angles, and the spread in incident photon energies, Figs.(1.25) and (1.26).